AIChE

Mechanism Studies on CVD of Boron Carbide from a Gas Mixture of BCl_3, CH_4, and H_2 in a Dual Impinging-jet Reactor

Mustafa Karaman
Dept. of Chemical Engineering, Middle East Technical University, Ankara 06531, Turkey
Dept. of Chemical Engineering, Selcuk University, Konya 42031, Turkey

Naime Aslı Sezgi, Timur Doğu, and Hilmi Önder Özbelge
Dept. of Chemical Engineering, Middle East Technical University, Ankara 06531, Turkey

DOI 10.1002/aic.11717
Published online February 2, 2009 in Wiley InterScience (www.interscience.wiley.com).

Nearly pure boron carbide free from impurities was produced on a tungsten substrate in a dual impinging-jet chemical vapor deposition reactor from a BCl_3, CH_4, and H_2 mixture. The Fourier Transform Infrared (FTIR) analysis proved the formation of reaction intermediate $BHCl_2$, which is proposed to occur mainly in the gaseous boundary layer next to the substrate surface. Among a large number of reaction mechanisms proposed only the ones considering the molecular adsorption of boron carbide on the substrate surface gave reasonable fits. In the proposed mechanism dichloroborane is formed in the gas phase only as a by-product. Boron carbide, on the other hand, is formed through a series of surface reactions involving adsorbed boron trichloride, adsorbed methane and gas phase hydrogen. The simultaneous fit of the experimental rate data to the model expressions gave correlation coefficient values of 0.977 and 0.948, in predicting the B_4C and $BHCl_2$ formation rates, respectively. *AIChE J,* 55: 701–709, 2009
Keywords: adsorption/gas, deposition methods (CVD, MOCVD), reaction kinetics

Introduction

Boron carbide is an important refractory carbide with excellent physical and chemical properties. Its high hardness, high melting point, high modulus of elasticity, large neutron capture section, low density and chemical inertness to most alkali and acids, make boron carbide a strong candidate for high technology applications.[1,2] Considering its high-temperature stability, large Seebeck coefficient and low thermal and high electrical conductivity, boron carbide could find potential use as high-temperature thermoelectric material for energy converters.[3] The need for a high quality boron carbide, especially for high technology applications, increased attention to study and develop novel boron carbide deposition techniques. Chemical vapor deposition (CVD) technique offers the advantage of a well controlled deposition of high purity single phase boron carbide.

Technical grade boron carbide (B_4C) can be deposited from various reaction gas mixtures over broad temperature and vapor composition ranges by the CVD method.[4] The deposition processes are carried out in excess hydrogen and the most commonly used boron and carbon precursors are BCl_3 and CH_4.[4–6]

Most of the previous studies on the CVD of boron carbide consider only the morphology of the deposited products.[4,5,7–9] A few studies involve the rate determination by classical

Correspondence concerning this article should be addressed to N. A. Sezgi at sezgi@metu.edu.tr.

thickness measurement of the deposits divided by the deposition time.[10,11] Vandenbulcke[6] deposited boron carbide from BCl_3-CH_4-H_2 mixture by using a stagnation flow technique in a cold wall reactor. A mass transfer equilibrium model was developed and this model was compared with the deposition rates and the solid compositions. The surface kinetics resistance was found to be an important factor since it limits the deposition rates. Santos et al.[11] proposed a mechanism change at 1050 K substrate temperature during laser assisted deposition of r-B_4C coatings using ethylene as carbon precursor, which was attributed to the change of rate controlling mechanism from the surface reaction kinetics to the mass transport of the gaseous species. Dilek et al.[12] studied only the effect of the inlet BCl_3 molar fraction on the reaction rates using methane as carbon precursor in a dual impinging-jet reactor where diffusion limitations were minimized. In our recent publication,[13] the effects of both BCl_3 and CH_4 inlet molar fractions on the reaction rates were investigated. Both dichloroborane and boron carbide formation rates were found to increase with an increase in the inlet molar fraction of BCl_3. However no effect on the formation rate of dichloroborane was observed while the formation rate of boron carbide increased with an increase in the inlet molar fraction of CH_4. There are a few published information related to the mechanism of CVD of boron carbide, which are not conclusive. Present study is a continuation of our earlier work[13] to find the mechanism of CVD of boron carbide from a reaction gas mixture of BCl_3, CH_4, and H_2. In this study, a detailed chemical investigation of CVD of boron carbide from the reaction gas mixture in an impinging-jet reactor was carried out to find a plausible reaction mechanism, to predict the formation rate of boron carbide, together with the rate of dichloroborane, which is the only stable intermediate observed in our system.

Experimental

To obtain reliable kinetic data and information about the reaction mechanism, minimization of transport limitations is quite important. Therefore a dual impinging-jet quartz reactor was constructed (Figure 1). The BCl_3, CH_4, and H_2 gas mixture, which was fed to the reactor through the two orifices in the middle of the reactor struck as a jet on to the both sides of the tungsten substrate, which hanged between two electrodes, upper one was fixed and the lower one was dipped into a mercury pool. The weight of the lower electrode kept the surface of the tungsten foil smooth and streched. The total volumetric flow rate of the gas mixture was kept constant at 200 cm^3/min in all experiments, which imposed a linear velocity of 2.1 m/s through each orifice. The substrate surface was heated to the desired temperature resistively by applying DC power through the electrodes. The temperature of the substrate surface was measured by an optical pyrometer. Details of the reaction system are published elsewhere.[13]

The on-line chemical analysis of the reactor outlet stream was carried out by an FTIR (PerkinElmer Spectrum One) spectrophotometer. Compositions of the reactor effluent were determined by calibrating the FTIR spectra for the reaction constituent gases according to the characteristic peak heights. The mole fraction ranges of methane and boron trichloride in the reactor inlet gas mixture were varied between 0.019–0.042 and 0.023–0.126, respectively, keeping a previously optimized substrate temperature of 1150°C at which rhombohedral boron carbide could be formed without any impurities.[13] During each run, the rate data was collected at different time intervals until steady state operation was reached.

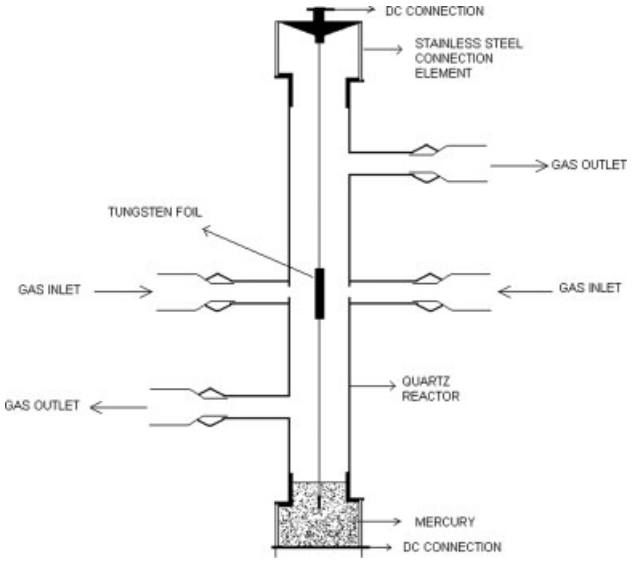

Figure 1. The dual impinging-jet CVD Reactor.

Results

The phase and composition analyses of the solid product were carried out by means of XRD and XPS methods in our previous study.[13] Within the range of inlet gas compositions studied, the formation of technical grade boron carbide (B_4C) was observed with carbon content around 17 at%, meaning that the product is within the homogeneity range of single stable phase boron carbide.[14] The formation of carbon, boron and any species (WB, WC) formed by an interaction of boron and carbon species with tungsten was not observed at 1150°C, at which the kinetic studies were carried out. In addition to this, the FTIR analysis of the reactor effluent stream showed that $BHCl_2$ and HCl were formed in the gas phase during the CVD of boron carbide from the BCl_3, CH_4, H_2 gas mixture.[13] The careful characterization studies of the produced solid phase together with the spectroscopic analysis of the reactor effluent revealed that two independent overall reactions must be enough to describe the CVD of boron carbide from the mixture of BCl_3, H_2, and CH_4 gases;

$$BCl_3(g) + H_2(g) + \tfrac{1}{4}CH_4(g) \Rightarrow \tfrac{1}{4}B_4C(s) + 3HCl(g) \qquad \text{(Reaction 1)}$$

$$BCl_3(g) + H_2(g) \Rightarrow BHCl_2(g) + HCl(g) \qquad \text{(Reaction 2)}$$

The following relations can be written between the observed rates of different species for this system:

$$R_{H_2} = +R_{BCl_3} \qquad R_{B_4C} = -R_{CH_4}$$

$$R_{BHCl_2} = +4R_{CH_4} - R_{BCl_3} \qquad R_{HC1} = -8R_{CH_4} - R_{BCl_3}$$

Mole fractions of reactor effluent gases were expressed in terms of fractional conversions to boron carbide(x_1) and dichloroborane(x_2). From the experimentally observed values of mole fractions of the reactor effluent gases, the conversion values of BCl_3 to B_4C (x_1), and to $BHCl_2$ (x_2), were calculated from the BCl_3 and CH_4 mole fraction equations. The mole fraction equations for H_2, BCl_3, CH_4, HCl, and $BHCl_2$ gases in terms of conversions were published elsewhere.[13] The rates of boron carbide and dichloroborane formation reactions were evaluated from the following equations

$$R_{B_4C} = A(R_{B_4C})_s = 1/4F_\circ y_{BCl_3o}x_1$$

$$R_{BHCl_2} = F_\circ y_{BCl_3o}x_2$$

where F_o is the total molar flow rate of the reactant stream and A is the surface area of the tungsten substrate that is in contact with the reactant gases within the reactor.

The major objective of using a dual impinging-jet reactor is to eliminate the mass transport effects and to obtain true kinetic data, which can also be used in the design of different CVD reactors. As it was discussed in our earlier publications,[15,16] the linear velocity of the jet at the orifice is 2.1 m/s and the distance between the orifice and the substrate surface is only 0.5 cm. In such a system mass transfer effects are expected to be minimized, if not totally eliminated. In fact our earlier studies had also shown that the conversion values obtained in this system were at least five times higher than the conversion values obtained for the same reaction in a parallel flow CVD reactor.[15,16] Significance of diffusional resistance in the parallel flow system and minimization of such effects in the impinging-jet reactor was also discussed in that earlier publications.[15,16]

The mechanism studies were carried out with the rate data for the samples that were produced at 1150°C. The effects of inlet boron trichloride and methane gases on the reaction rates at this temperature are shown in Figure 2. The rate of boron carbide formation reaction increases up to a certain value of boron trichloride mole fraction, and then reaches a plateau and remains nearly constant. This result may be the indication of an adsorption of BCl_3 molecules on the surface. This observation is also consistent with the study of Sezgi[16] in which boron deposition was considered to take place in a mechanism involving non-dissociative adsorption of boron trichloride molecules on the substrate surface. As shown in Figure 2, the rate of dichloroborane increases with an increase in the mole fraction of boron trichloride. This behavior of the rate data may be due to the $BHCl_2$ formation reaction taking place mainly in the gas phase within the thin thermal boundary layer next to the substrate surface.

A large number of reaction mechanisms consisting of different types of elementary reaction steps, involving various types of surface reactions leading to B_4C and $BHCl_2$ formations, totally gas phase reaction, adsorption of reactant gases on the surface, surface reactions and desorption of reaction products from the surface were proposed to predict the formation rates of boron carbide and dichloroborane simultaneously. The rate expressions for formations of boron carbide and dichloroborane were derived from the proposed mechanisms and tested with the independent experimental rate data

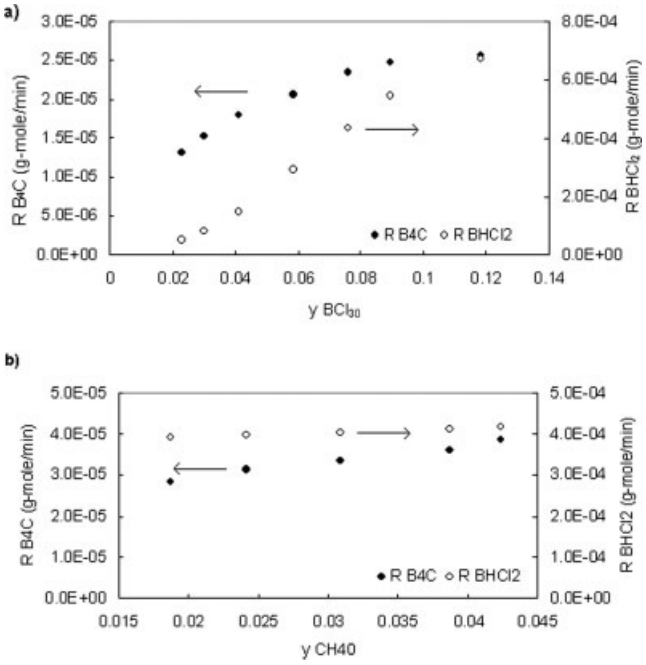

Figure 2. Effects of inlet molar fractions of (a) BCl_3 ($y_{CH_{40}}$ = 0.02) and (b) CH_4 ($y_{BCl_{30}}$ = 0.084) on the formation rates of boron carbide and dichloroborane (T = 1150°C, in excess hydrogen).

using non-linear regression analysis. In the non-linear regression analysis, Pearson product moment correlation coefficient was used. The formula of correlation coefficient (r) is $\frac{1}{n-1}\sum_{i=1}^{n}\left(\frac{X_i-\bar{X}}{s_X}\right)\left(\frac{Y_i-\bar{Y}}{s_Y}\right)$ where X, Y are the experimental rate data and model rate data obtained from the proposed mechanism, respectively. In the program, iteration, step size and tolerance values were set and then, the rate data and rate equations for boron carbide and $BHCl_2$ formation reactions and the initial values for each parameter were entered the program. The program finds the same parameters whatever the initial parameter values are. After regression process, the proposed mechanisms should predict both rates with an acceptable accuracy. Moreover, many of the mechanisms contained some common rate parameters appearing in the rate expressions. So, the data for the boron carbide and dichloroborane formation rates were simultaneously analyzed to predict a reaction mechanism.

The various combinations of possible elementary reaction steps, together with the selection of the rate determining step among the elementary steps, are the factors that make the difference between the mechanisms. Some of the most probable elementary reaction steps considered for this system are shown in Table 1.

In the derivation of the rate expressions, the only adsorbed species were taken as BCl_3, H_2, and CH_4. The adsorption terms for the product gases HCl and $BHCl_2$ were not considered because such species were swept away from the surface during the impingement of the reactant gases to the substrate surface.

Table 1. Probable Surface Reaction Steps Taking Place in the CVD of Boron Carbide from a BCl_3, H_2, and Ch_4 Mixture

Adsorption Reactions		Surface Reactions for Boron Carbide Formation	
$BCl_3 + s \leftrightarrow s.BCl_3$ (nondissociative)	a1	$s.BC + BCl_3 + H_2 + s \rightarrow s.B_2C + 2HCl + s.Cl$	b1
$BCl_3 + 2s \rightarrow s.BCl_2 + s.Cl$ (dissociative)	a2	$s.B_2C + BCl_3 + H_2 + s \rightarrow s.B_3C + 2HCl + s.Cl$	b2
$BCl_3 + 3s \rightarrow s.BCl + 2s.Cl$ (pyrolytic)	a3	$s.B_3C + BCl_3 + H_2 + s \rightarrow s.B_4C + 2HCl + s.Cl$	b3
$CH_4 + s \leftrightarrow s.CH_4$ (nondissociative)	a4	$s.BC + s.BCl + H_2 \rightarrow s.B_2C + s.H + HCl$	b4
$CH_4 + 2s \leftrightarrow s.CH_3 + s.H$ (dissociative)	a5	$s.B_2C + s.BCl + H_2 \rightarrow s.B_3C + s.H + HCl$	b5
$H_2 + 2s \leftrightarrow 2s.H$ (dissociative)	a6	$s.B_3C + s.BCl + H_2 \rightarrow s.B_4C + s.H + HCl$	b6
		$s.BCl + s.C + H_2 \rightarrow s.BC + s.H + HCl$	b7
Surface reactions for BCl_3 decomposition		$s.BC + s.BCl_3 + H_2 \rightarrow s.B_2C + 2HCl + s.Cl$	b8
$s.BCl_3 + H_2 \rightarrow s.BCl + 2HCl$	c1	$s.B_2C + s.BCl_3 + H_2 \rightarrow s.B_3C + 2HCl + s.Cl$	b9
$s.BCl_3 + s.H \rightarrow s.BCl_2 + s.HCl$	c2	$s.B_3C + s.BCl_3 + H_2 \rightarrow s.B_4C + 2HCl + s.Cl$	b10
$s.BCl_3 + s \rightarrow s.BCl_2 + s.Cl$	c3	$CH_4 + s \rightarrow s.C + 2H_2$	b11
$s.BCl_2 + s.H \rightarrow s.BCl + s.HCl$	c4	$s.BHC + BCl_3 + H_2 \rightarrow s.B_2C + 3HCl$	b12
$s.BCl + CH_4 \rightarrow s.BC + HCl + 3/2H_2$	c5	$s.BC + BCl_3 + 3/2\ H_2 \rightarrow s.B_2C + 3HCl$	b13
$s.BCl_3 + CH_4 \rightarrow s.BC + 3HCl + 1/2H_2$	c6	$s.B_2C + BCl_3 + 3/2\ H_2 \rightarrow s.B_3C + 3HCl$	b14
$s.BCl_3 + CH_4 \rightarrow s.BHC + 3HCl$	c7	$s.B_3C + BCl_3 + 3/2\ H_2 \rightarrow s.B_4C + 3HCl$	b15
$BCl_3 + s.CH_3 \rightarrow s.BC + 3HCl$	c8		
$s.BCl_3 + s.CH_3 \rightarrow s.BC + 3HCl + s$	c9	Desorption reactions	
$s.BCl_3 + s.C + 2H_2 \rightarrow s.BC + 3HCl + s.H$	c10	$s.BHCl_2 \rightarrow BHCl_2 + s$	e1
		$s.HCl \rightarrow HCl + s$	e2
$BHCl_2$ formation		$s.BCl_2 \rightarrow BCl_2 + s$	e3
$s.BCl_3 + H_2 + ns \rightarrow s.BHCl_2 + s.HCl + (n-1)s$	d1	$s.BCl \rightarrow BCl + s$	e4
$s.BCl_3 + 2(s.H) \rightarrow s.BHCl_2 + s.HCl + s$	d2	Decomposition of $BHCl_2$	
$s.BCl_2 + s.H \rightarrow s.BHCl_2 + s$	d3	$s.BHCl_2 + s \rightarrow s.BCl_2 + s.H$	f1
$s.BCl_3 + 2(s.H) \rightarrow BHCl_2 + HCl + 3s$	d4	$s.BHCl_2 + s.BCl_3 \rightarrow 2(s.BCl_2) + HCl$	f2
		$s.BHCl_2 + s.H + s \rightarrow s.B + 2(s.HCl)$	f3

s is a surface site (boron carbide).

BCl_3 adsorption on the substrate surface may be nondissociative, partially dissociative or completely dissociative (Table 1, a1–a3). Other reaction precursors, methane and hydrogen, may or may not adsorb on the surface, and react with adsorbed boron trichloride molecule through Langmuir Hinshelwood or Rideal Eley type of surface reactions (b1–b11, c1–c10). Hydrogen adsorption was considered to be dissociative (a6) at the substrate temperature studied, however methane adsorption could be nondissociative (a4), or dissociative (a5). Free adsorbed carbon atoms may form with the reaction of the methane gas and vacant surface site (b11) and they then may react with adsorbed boron trichloride molecule to start the formation of boron carbide (b7, c10). Some possible surface reaction steps for the $BHCl_2$ formation are given in Table 1 (d1–d3). At high temperatures, adsorbed $BHCl_2$ molecule may further decompose (f1–f3).

Among the extensive number of the mechanisms considered, only the ones in which adsorption of boron trichloride on the surface was included in the mechanisms (a1) gave reasonable fits for the boron carbide formation rate data. The almost linear increase of the dichloroborane formation rate with initial boron trichloride molar fraction may be an indication of the dichloroborane formation reaction taking place mainly in gas phase. Modelling studies revealed that, the mechanisms in which dichloroborane formation reaction was considered to take place only in gas phase, gave very good fits, for the formation rates of both species. On the other hand, models containing surface reaction steps in addition to the gas phase formation reaction for dichloroborane formation (d1–d3), gave poor fits, especially to predict the deposition rate of boron carbide. Moreover, according to the subsequent curve fitting process, the gas phase reaction of dichloroborane formation should be elementary and first order with respect to BCl_3 concentration. Since the hydrogen participates in reaction, one would expect the rate law to have the form of $r = P_{BCl_3} P_{H_2}$. Because hydrogen is always present in great excess, its concentration remains essentially constant in a given run. Therefore hydrogen was excluded from the rate law and the reaction becomes pseudo first order. In spite of the absence of any decomposition products of $BHCl_2$ on the solid phase, further dissociation of dichloroborane (f1–f3) was considered in some models and as expected the mechanisms involving such reactions were poor in the prediction of the experimental rate data. Models in which the hydrogen did not adsorb were poor in the prediction of the experimental rate data.

Boron carbide formation reaction was considered to take place through successive series reactions, in which boron and carbon atoms are incorporated into the solid structure to form boron carbide finally (b1–b10). B_2C, B_3C, BC, and BHC are expected to be very reactive and the fraction of the surface covered by these species is most likely very low. Therefore, steady state approximation was applied for the boron-carbon containing intermediates appearing in the successive series reactions.

Adsorbed boron trichloride further decomposes through surface reactions involving the reaction of adsorbed BCl_3 with either gas phase hydrogen and methane (c1, c5–c7), or adsorbed hydrogen (c2), and adsorbed methane (c9).

An extensive number of mechanisms involving different combinations of elementary reaction steps given in Table 1 and different types of rate determining steps were considered in simultaneous analysis of rate data for boron carbide and dichloroborane formation reactions. The best three reaction models are summarized below and a list of some of the reac-

Table 2. Rate Expressions which Gave Poor Fit

Model	Rate Expressions	Rate Parameters	Correlation Coefficients for R_{B_4C}	Correlation Coefficients for R_{BHCl_2}
$BCl_3 + 2s \xrightarrow{k_{a2}} sBCl_2 + sCl$ $H_2 + 2s \xleftrightarrow{K_{a6}} 2sH$ $sBCl_2 + sH \xrightarrow{k_6} sBCl + HCl + s$ $sBCl + CH_4 \xrightarrow{k_{c5}} sBC + HCl + 3/2H_2$ $sBC + BCl_3 + H_2 + s \xrightarrow{k_{b1}} sB_2C + 2HCl + sCl$ $sB_2C + BCl_3 + H_2 + s \xrightarrow{k_{b2}} sB_3C + 2HCl + sCl$ $sB_3C + BCl_3 + H_2 + s \xrightarrow{k_{b3}} sB_4C + 2HCl + sCl$ $sH + sCl \xrightarrow{k_5} HCl + 2s$ $sBCl_2 + sH \xrightarrow{k_{d3}} sBHCl_2 + s$ $sBHCl_2 \xrightarrow{k_{e1}} BHCl_2 + s$ $BCl_3 + H_2 \xrightarrow{k_g} BHCl_2 + HCl$	$R_{B_4C} = \frac{DP_{BCl_3}}{\left(1 + E\frac{P_{BCl_3}}{P_{H_2}^{1/2}} + (K_{a6}P_{H_2})^{1/2}\right)^2}$ $R_{BHCl_2} = \frac{FP_{BCl_3}}{\left(1 + E\frac{P_{BCl_3}}{P_{H_2}^{1/2}} + (K_{a6}P_{H_2})^{1/2}\right)^2} + k_g P_{BCl_3} P_{H_2}$	$D = \frac{k_{a2}k_6}{k_6 + k_{d3}} = 31.1$ $E = \frac{k_{a2}}{(k_6 + k_{d3})K_{a6}^{1/2}} = 4.69 * 10^{-8}$ $K_{a6} = 472.82$ $F = \frac{k_{d3}}{k_6 + k_{d3}} = 472.8$ $k_g = 2.73*10^{-14}$	0.470	0.961
$BCl_3 + s \xleftrightarrow{K_{a1}} sBCl_3$ $sBCl_3 + CH_4 \xleftrightarrow{K_{c6}} sBC + 3HCl + 1/2H_2$ $sBC + BCl_3 + 3/2H_2 \xrightarrow{k_{b13}} sB_2C + 3HCl$ $sB_2C + BCl_3 + 3/2H_2 \xrightarrow{k_{b14}} sB_3C + 3HCl$ $sB_3C + BCl_3 + 3/2H_2 \xrightarrow{k_{b15}} sB_4C + 3HCl$ $sBCl_3 + H_2 \xleftrightarrow{K_6} sBHCl_2 + HCl$ $sBHCl_2 \xrightarrow{k_{e1}} BHCl_2 + s$ $BCl_3 + H_2 \xrightarrow{k_g} BHCl_2 + HCl$	$R_{B_4C} = \frac{DP_{CH_4}P_{BCl_3}^2P_{H_2}}{P_{HCl}^3(1 + K_{a1}P_{BCl_3})}$ $R_{BHCl_2} = \frac{FP_{H_2}P_{BCl_3}}{P_{HCl}(1 + K_{a1}P_{BCl_3})} + k_g P_{BCl_3} P_{H_2}$	$D = k_{b13}\,K_{a1}\,K_{c6} = 5.3*10^{-5}$ $F = k_{e1}K_{a1}K_6 = 1.63*10^{-12}$ $K_{a1} = 5.8*10^{-3}$ $k_g = 2.71*10^{-7}$	–	0.945
$BCl_3 + s \xleftrightarrow{K_{a1}} sBCl_3$ $H_2 + 2s \xleftrightarrow{K_{a6}} 2sH$ $sBCl_3 + CH_4 \xrightarrow{k_{c6}} sBC + 3HCl + 1/2H_2$ $sBC + BCl_3 + H_2 + s \xrightarrow{k_{b1}} sB_2C + 2HCl + sCl$ $sB_2C + BCl_3 + H_2 + s \xrightarrow{k_{b2}} sB_3C + 2HCl + sCl$ $sB_3C + BCl_3 + H_2 + s \xrightarrow{k_{b3}} sB_4C + 2HCl + sCl$ $sH + sCl \xrightarrow{k_5} HCl + 2s$ $sBCl_3 + 2sH \xrightarrow{k_{d4}} BHCl_2 + HCl + 3s$ $BCl_3 + H_2 \xrightarrow{k_g} BHCl_2 + HCl$	$R_{B_4C} = \frac{DP_{CH_4}P_{BCl_3}}{\left(1 + K_{a1}P_{BCl_3} + (K_{a6}P_{H_2})^{1/2}\right)}$ $R_{BHCl_2} = \frac{FP_{H_2}P_{BCl_3}}{P_{HCl}\left(1 + K_{a1}P_{BCl_3} + (K_{a6}P_{H_2})^{1/2}\right)} + k_g P_{BCl_3} P_{H_2}$	$D = k_{c6}K_{a1} = 2.85$ $K_{a1} = 2.0*10^{-5}$ $K_{a6} = 57343$ $F = k_{d4}K_{a1}K_{a6} = 53413$ $k_g = 1.21*10^{-3}$	0.632	0.956

Table 2. (*Continued*)

Model	Rate Expressions	Rate Parameters	Correlation Coefficients for R_{B_4C}	Correlation Coefficients for R_{BHCl_2}
$BCl_3+s \overset{K_{a1}}{\longleftrightarrow} sBCl_3$ $H_2+2s \overset{K_{a6}}{\longleftrightarrow} 2sH$ $sBCl_3+CH_4 \overset{k_{c6}}{\longrightarrow} sBC+3HCl+1/2H_2$ $sBC+BCl_3+3/2H_2 \overset{k_{b13}}{\longrightarrow} sB_2C+3HCl$ $sB_2C+BCl_3+3/2H_2 \overset{k_{b14}}{\longrightarrow} sB_3C+3HCl$ $sB_3C+BCl_3+3/2H_2 \overset{k_{b15}}{\longrightarrow} sB_4C+3HCl$ $sBCl_3+H_2+s \overset{k_{d1}}{\longrightarrow} sBHCl_2+sHCl$ $sBHCl_2+ \overset{k_{e1}}{\underset{k_g}{\longrightarrow}} BHCl_2+s$ $BCl_3+H_2 \overset{k_g}{\longrightarrow} BHCl_2+HCl$	$R_{B_4C} = \frac{DP_{CH_4}P_{BCl_3}}{\left(1+K_{a1}P_{BCl_3}+(K_{a6}P_{H_2})^{1/2}\right)}$ $R_{BHCl_2} = \frac{FP_{H_2}P_{BCl_3}}{\left(1+K_{a1}P_{BCl_3}+(K_{a6}P_{H_2})^{1/2}\right)^2} + k_gP_{BCl_3}P_{H_2}$	$D = K_{a1}k_{c6} = 0.053$ $K_{a1} = 37.87$ $K_{a6} = 1.8*10^{-11}$ $F = k_{d1}K_{a1} = 5.88*10^{-3}$ $k_g = 1.09*10^{-4}$	0.8	0.944
$BCl_3+s \overset{K_{a1}}{\longleftrightarrow} sBCl_3$ $H_2+2s \overset{K_{a6}}{\longleftrightarrow} 2sH$ $CH_4+s \overset{k_3}{\longrightarrow} sCH_3+1/2H_2$ $BCl_3+sCH_3 \overset{k_{c8}}{\longrightarrow} sBC+3HCl$ $sBC+BCl_3+H_2+s \overset{k_{b1}}{\longrightarrow} sB_2C+2HCl+sCl$ $sB_2C+BCl_3+H_2+s \overset{k_{b2}}{\longrightarrow} sB_3C+2HCl+sCl$ $sB_3C+BCl_3+H_2+s \overset{k_{b3}}{\longrightarrow} sB_4C+2HCl+sCl$ $sH+sCl \overset{k_5}{\longrightarrow} HCl+2s$ $sBCl_3+H_2+s \overset{k_{d1}}{\longrightarrow} sBHCl_2+sHCl$ $sBHCl_2 \overset{k_{e1}}{\underset{k_g}{\longrightarrow}} BHCl_2+s$ $BCl_3+H_2 \overset{k_g}{\longrightarrow} BHCl_2+HCl$	$R_{B_4C} = \frac{k_3P_{CH_4}P_{BCl_3}}{\left(1+K_{a1}P_{BCl_3}+D\frac{P_{CH_4}}{P_{BCl_3}}+(K_{a7}P_{H_2})^{1/2}\right)}$ $R_{BHCl_2} = \frac{FP_{H_2}P_{BCl_3}}{\left(1+K_{a1}P_{BCl_3}+D\frac{P_{CH_4}}{P_{BCl_3}}+(K_{a7}P_{H_2})^{1/2}\right)} + k_gP_{BCl_3}P_{H_2}$	$k_3 = 2.656$ $K_{a1} = 5.84*10^{-6}$ $D = \frac{k_3}{k_{c8}} = 154.9$ $K_{a7} = 26670$ $F = k_{d1}K_{a1} = 1.167$ $k_g = 2.035*10^{-10}$	0.643	0.962
$BCl_3+s \overset{K_{a1}}{\longleftrightarrow} sBCl_3$ $H_2+2s \overset{K_{a6}}{\longleftrightarrow} 2sH$ $CH_4+2s \overset{K_{a5}}{\longleftrightarrow} sCH_3+sH$ $sBCl_3+sCH_3 \overset{k_{c9}}{\longrightarrow} sBC+3HCl+s$ $sBC+sBCl_3+H_2 \overset{k_{b8}}{\longrightarrow} sB_2C+2HCl+sCl$ $sB_2C+sBCl_3+H_2 \overset{k_{b9}}{\longrightarrow} sB_3C+2HCl+sCl$ $sB_3C+sBCl_3+H_2 \overset{k_{b10}}{\longrightarrow} sB_4C+2HCl+sCl$ $sBCl_3+H_2 \overset{k_7}{\longrightarrow} BHCl_2+HCl+s$ $BCl_3+H_2 \overset{k_g}{\longrightarrow} BHCl_2+HCl$	$R_{B_4C} = \frac{DP_{CH_4}P_{BCl_3}}{P_{H_2}^{1/2}\left(1+K_{a1}P_{BCl_3}+E\frac{P_{CH_4}}{P_{H_2}^{1/2}}+(K_{a2}P_{H_2})^{1/2}\right)^2}$ $R_{BHCl_2} = \frac{FP_{H_2}P_{BCl_3}}{\left(1+K_{a1}P_{BCl_3}+E\frac{P_{CH_4}}{P_{H_2}^{1/2}}+(K_{a2}P_{H_2})^{1/2}\right)} + k_gP_{BCl_3}P_{H_2}$	$D = \frac{k_{c9}K_{a5}K_{a1}}{K_{a2}^{1/2}} = 617.2$ $K_{a1} = 1.02*10^{-5}$ $E = \frac{K_{a5}}{K_{a2}^{1/2}} = 303.8$ $K_{a2} = 53564$ $F = k_7K_{a1} = 68111$ $k_g = 3.92*10^{-10}$	0.634	0.962

Table 3. The Best Three Models for the CVD of B_4C from CH_4, H_2, and BCl_3 mixture at 1150°C

Model	Rate Expressions	Rate Parameters	Correlation Coefficients for R_{B_4C}	Correlation Coefficients for R_{BHCl_2}
A	$R_{B_4C} = \frac{DP_{CH_4}P_{BCl_3}}{P_{H_2}^{1/2}\left(1 + K_{a1}P_{BCl_3} + E\frac{P_{CH_4}}{P_{H_2}^{1/2}}\right)^2}$	$D = \frac{k_{c9}K_{a5}K_{a1}}{K_{a6}^{1/2}} = 0.0682$ $K_{a1}=9.36$ $E = \frac{K_{a5}}{K_{a6}^{1/2}} = 18.47$	0.977	0.948
	$R_{BHCl_2} = k_gP_{BCl_3}$	$k_g=0.00521$		
B	$R_{B_4C} = \frac{DP_{CH_4}P_{BCl_3}}{(1 + K_{a1}P_{BCl_3} + EP_{H_2}^{1/2})^2}$	$D=k_{c7}K_{a6}=46.65$ $K_{a1}=338.3$ $E=K_{a6}^{1/2} = 33.3$	0.832	0.946
	$R_{BHCl_2} = \frac{FP_{CH_4}P_{BCl_3}}{(1 + K_{a1}P_{BCl_3} + EP_{H_2}^{1/2})^2} + k_gP_{BCl_3}$	$F=k_{d1}K_{a1} = 2.55*10^{-4}$ $k_g=0.0055$		
C	$R_{B_4C} = \frac{DP_{CH_4}P_{BCl_3}P_{H_2}^{3/2}}{(1 + K_{a1}P_{BCl_3} + FP_{H_2}^{1/2})^2}$	$D=k_{b11}k_{c10}K_{a1}=60.3$ $K_{a1}=302.0$	0.754	0.955
	$R_{BHCl_2} = \frac{GP_{H_2}P_{BCl_3}}{(1 + K_{a1}P_{BCl_3} + FP_{H_2}^{1/2})^3} + k_gP_{BCl_3}$	$F=K_{a6}^{1/2} = 38.58$ $G=k_{d4}K_{a1}K_{a6}=3.6*10^{-3}$ $k_g=5.2*10^{-3}$		

K_{a1}, K_{a5}, and K_{a6} are the adsorption equilibrium constants for BCl_3 (a1), CH_4 (a5), H_2 (a6); k_{b11}, k_{c7}, k_{c9}, k_{c10}, k_{d1}, and k_{d4} are the rate constants for reactions b11, c7, c9, c10, d1, and d4, respectively. kg is the rate constant of the gas phase formation reaction of $BHCl_2$.

tion models that were tested but did not work is tabulated in Table 2. The rate expressions that are derived from the best three models and the rate parameters obtained from simultaneous analyses of R_{B_4C} and R_{BHCl_2} data by nonlinear multiple regression analysis are given in Table 3. The comparison of the experimental and model predicted values of the boron carbide and dichloroborane formation rates is illustrated in Figure 3.

Model A

In this model, boron trichloride is adsorbed on the surface non-dissociatively (a1), whereas methane and hydrogen are adsorbed dissociatively (a5, a6). Adsorbed boron trichloride is decomposed through a Langhmiur-Hinshelwood type of a surface reaction with dissociatively adsorbed methane ($s.CH_3$) (c9). Boron carbide is formed on the solid surface through the series reactions (b8–b10), in which boron atom is incorporated to the solid structure in each step. Steady-state approximation was applied for the adsorbed intermediates appearing in reactions c9, b8, and b9. In the proposed model, dichloroborane formation reaction was considered to take place only through gas phase reaction of boron trichloride with hydrogen. Gaseous hydrogen chloride is produced through a surface reaction of adsorbed hydrogen and adsorbed chlorine. In fact this model gives the highest correlation coefficient values in the models that considers only gas phase formation of dichloroborane. The simultaneous fit of the experimental data to the model expressions gave the highest correlation coefficient of 0.977, in fitting the B_4C formation rate data. Estimated model parameters together with the statistical correlation coefficients are summarized in Table 3.

Model B

In this model, the boron trichloride and hydrogen gases are adsorbed on the solid surface through reactions a1 and a6. Then the adsorbed boron trichloride reacts with gaseous methane through a Rideal-Eley type surface reaction (c7) to produce adsorbed intermediate species BHC. Boron is added to structure in the successive reactions involving gaseous boron trichloride, adsorbed B_2C or adsorbed B_3C species and hydrogen (b12, b2–b3). In each successive reaction, HCl gas is produced as a by-product. The rate determining step for boron carbide deposition was taken as (b3). The rate determining step of $BHCl_2$ formation involves reaction between adsorbed boron trichloride and hydrogen (d1). Adsorbed dichloroborane is then desorbed back to the gaseous phase through reaction e1. In this model, dichloroborane is produced by two competing mechanism; first one is the surface reaction described above and the second one is the contribution of gas phase formation reaction through reduction of BCl_3 by H_2. Hydrogen chloride is produced through the surface reaction of adsorbed hydrogen and adsorbed chlorine. The simultaneous analysis of the rate expressions derived from the model with the experimental data predicted the boron trichloride effect on the formation rate of boron carbide well for low inlet BCl_3 molar fractions. However at high BCl_3 inlet concentrations, the model failed (Figure 3). The rate parameters together with the corresponding *r* values for the model are given in Table 3. This model is not enough to describe the observed behavior considering the low correlation coefficient for the B_4C formation reaction (Table 3).

Model C

In this model, the boron trichloride and hydrogen gases are adsorbed on the solid surface through reactions a1 and a6

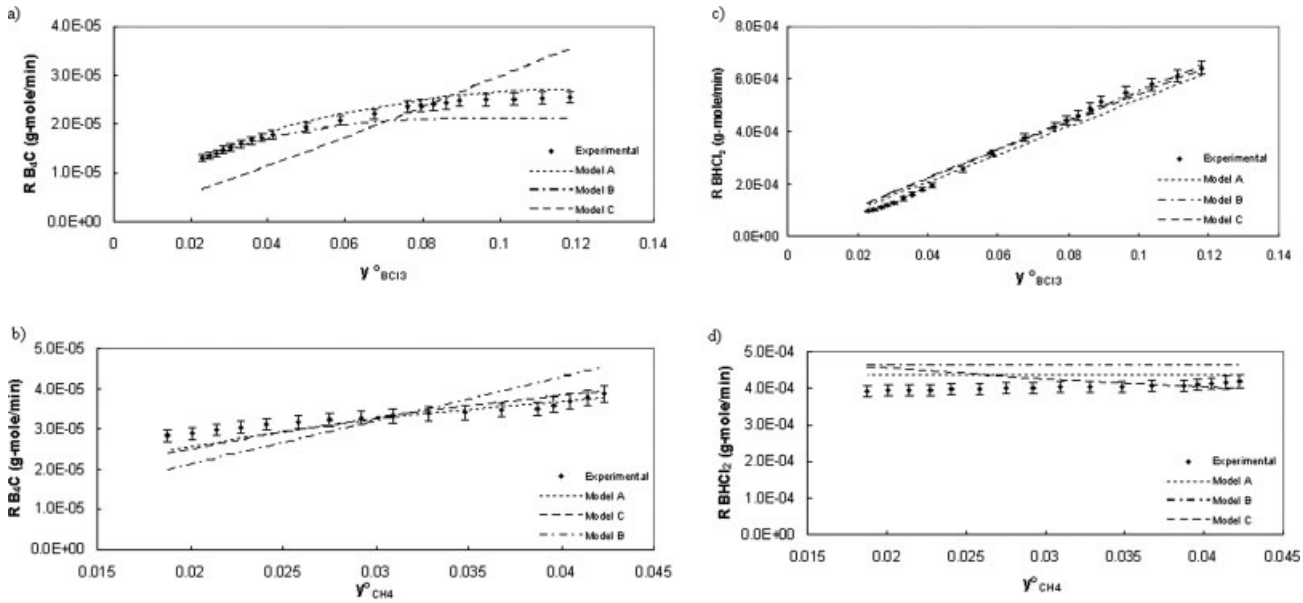

Figure 3. Comparison of rate data with model predictions for boron carbide and dichloroborane formation reactions at 1150°C and different initial mole fractions of boron trichloride (a, b) and methane (c, d) in excess hydrogen.

as in Model A and B. The gas phase methane reacts with a vacant surface site to produce adsorbed carbon (b11). The adsorbed carbon is reacted with adsorbed boron trichloride to form adsorbed BC species (c10), which then reacts with gaseous boron trichloride and hydrogen, in successive steps (b13–b15), to obtain boron carbide. The dichloroborane formation occurs again in two steps. In contrast to the previous mechanism, here dichloroborane is formed through a Langmuir Hinshelwood type of reaction kinetics through the reaction of adsorbed boron trichloride and adsorbed hydrogen (d2) in addition to the gas phase formation reaction. The model rate expressions derived for this model are given in Table 3. The simultaneous fit of the experimental data to the derived rate expressions gave poor fit for the formation of boron carbide (Figure 3a). For dichloroborane formation, model predictions are in acceptable agreement with the experimental data, with an r value of 0.955 (Table 3).

It is evident from Figure 3 that, the experimental data was best described by model A. This model predicts the deposition rate of B_4C and $BHCl_2$ well for the entire range of parameters studied. The model does not consider the probable surface reactions in the formation of $BHCl_2$, and hence formation rate is independent of methane partial pressure. This is also met by the experimental observation in which dichloroborane formation rate is almost unchanged with the variation of the initial methane mole fraction.

Conclusions

The FTIR analysis of the reactor effluent stream showed that $BHCl_2$ was formed as the only stable intermediate during the CVD of boron carbide from the BCl_3, CH_4, H_2 gas mixture. The formation of $BHCl_2$ was attributed mainly to the gas phase reaction within the thin thermal boundary layer next to the substrate surface. The poor fits of the reaction models which consider the formation of $BHCl_2$ through heterogeneous surface reactions support the idea of gas phase formation of that intermediate. Among a large number of reaction mechanisms proposed only the ones considering molecular adsorption of boron carbide on the substrate surface gave reasonable fits. Hydrogen and methane, on the other hand should be dissociatively adsorbed on the substrate surface, to obtain a good fit. In the proposed model, the adsorbed intermediates, together with the gas phase hydrogen, are reacted in successive series reactions to produce finally stoichiometric B_4C phase. The mechanism that involves foregoing elementary steps (Model A) is quite satisfactory to predict the deposition rates of boron carbide and dichloroborane simultaneously.

Acknowledgments

The authors thank to The Scientific and Technological Research Council of Turkey (TUBITAK) (project no: Misag-217) and State Planning Organization of Turkey (project no: BAP-08-11-DPT2002K120510-IM-5) for their financial supports of this project.

Notation

A = reaction surface area (mm^2)
E_a = activation energy (kjoule/mol)
F_o = molar flow rate of the reactant stream (mol/min)
k_o = frequency factor (mol/min)
R = gas constant (kjoule/mol-K)
R_s = reaction rate based on the unit surface area of the substrate (mole/min-mm^2)
R = reaction rate based on the surface area of the filaments (mole/min)
s = standard deviation
T = temperature (K)
X = experimental rate data
Y = model rate data obtained from the proposed mechanism

$\bar{X}$, $\bar{Y}$ = mean
x_1 = fractional conversion of BCl_3 to B_4C
x_2 = fractional conversion of BCl_3 to $BHCl_2$
y_i = mole fraction of component i

Literature Cited

1. Sezer AO, Brand JI. Chemical vapor deposition of boron carbide. *Mater Sci Eng*. 2001;B79:191–202.
2. Thevenot F. Boron carbide-A comprehensive review. *J Eur Ceram Soc*. 1990;6:205–225.
3. Oliviera JC, Conde O. Deposition of boron carbide by laser CVD: a comparison with thermodynamic predictions. *Thin Solid Films*. 1997;307:29–37.
4. Cansson U, Carlsson JO, Stridh B, Söderberg S, Olsson M. Chemical vapor deposition of boron carbides I: phase and chemical composition. *Thin Solid Films*. 1989;172:81–93.
5. Oliviera JC, Oliviera MN, Conde O. Structural characterization of B_4C films deposited by laser-assisted CVD. *Surf Coat Technol*. 1996;80:100–104.
6. Vandenbulcke LG. Theoretical and experimental studies on the chemical vapor deposition of boron carbide. *Ind Eng Chem Res*. 1985;24:568–575.
7. Cochran AA, Stephenson JB. Boron and boron carbide coatings by vapor deposition. *Metallurg Trans*. 1970;1:2875–2877.
8. Desphande SV, Gulari E, Harris SJ, Weiner AM. Filament activated chemical vapor deposition of boron carbide coatings. *Appl Phys Lett*. 1994;65:1757–1759.
9. Ploog K. Composition and structure of boron carbides prepared by CVD. *J Cryst Growth*. 1974;24/25:197–204.
10. Grigorev YM, Zharkov AV, Mukasyan AS, Shugaev VA. Macrokinetic relationships in forming boron carbide fibers by chemical vapor deposition. *Neorganicheskie Materialy*. 1993;29:344–348.
11. Santos MJ, Silvestre AJ, Conde O. Laser-assisted deposition of r-B_4C coatings using ethylene as carbon precursor. *Surf Coat Technol*. 2002;151–152:160–164.
12. Dilek SN, Özbelge HÖ, Sezgi NA, Doğu T. Kinetic studies for boron carbide in a dual impinging-jet reactor. *Ind Eng Chem Res*. 2001;40:751–755.
13. Karaman M, Sezgi NA, Dogu T, Ozbelge HO. Kinetic investigation of chemical vapor deposition of B_4C on tungsten substrate. *AICHE J*. 2006;52:4161–4166.
14. Tallant DR, Aselage TL, Campbell AN, Emin D. Boron carbides: Evidence for molecular level disorder. *J Non-Cryst Solids*. 1988;106:370–373.
15. Sezgi NA, Ersoy A, Dogu T, Ozbelge HO. CVD of boron and dichloroborane formation in a hot-wire fiber growth reactor. *Chem Eng Process*. 2001;40:525–530.
16. Sezgi NA, Dogu T, Ozbelge HO. Mechanism of CVD of boron by hydrogen reduction of BCl_3 in a dual impinging-jet reactor. *Chem Eng Sci*. 1999;54:3297–3304.

Manuscript received Apr. 8, 2008, revision received July 28, 2008, and final revision received Sept. 26, 2008.